Numerical simulation of the pinching of partially neutralized relativistic electron beams

G. Martínez* and R. Becker
Institut für Angewandte Physik der J. W. Goethe-Universität Frankfurt am Main, Robert-Mayer-Straße 2-4, D-60054 Frankfurt, Germany
(Received 31 March 2000; published 6 October 2000)

The compression of relativistic electron beams resulting from partial space charge neutralization by thermal ions is simulated to obtain self-consistent solutions. The numerical modeling is based on a finite difference approach, using under-relaxation to assure convergence in solving this nonlinear problem. The results show a nonuniform fraction of neutralization, increasing as a function of radius. Neutralization on axis is higher for colder compensating ions and for lower electron energy. In general, the temperature of the ions turns out to be higher than that of the electrons. With respect to the non-neutralized, not-thermally-dispersed beam, higher compression factors result at higher beam energies. The analytic solutions, known as the Bennett pinch, are well matched at corresponding settings of the parameters.

PACS numbers: 41.75.Ht, 41.20.Cv, 41.85.Ew, 07.05.Tp

I. INTRODUCTION

Electron beams without external focusing are found in several applications: electron beam welding, x-ray tomography scanners, and special kinds of electron beam ion sources and traps (EBIS and EBIT). The propagation of these beams is determined by their self-electric and self-magnetic fields, causing beam spreading by space charge, its reduction by ion neutralization, and additional focusing by pinching at relativistic energies. For the modeling of the behavior of thermal electrons and thermal ions, self-consistent solutions are required for the radial distribution functions. In general, it is necessary to find these by applying numerical techniques, although some simple cases can be solved analytically.

As early as 1934, Bennett [1] gave the classical treatment for the neutralization of a relativistic electron beam by ions, with transverse Maxwellian distribution of velocities for both kinds of particles. He found particular solutions for the radial variation of charges, based on a constant (as a function of radius) degree of neutralization f. In a paper by Budker [2] the stability of pinched beams is discussed. Lawson [3] is reporting more analytic approaches to other configurations, still based on a constant f. A nonuniform radial neutralization resulted from the treatment by Rand *et al.* [4], neglecting, however, thermalizing collisions between the ions. This is restricted to the case where the thermalization time is much longer than the time for neutralization. Only more recently, thermal distributions for electrons and ions have been taken into account in numerical calculations of neutralization [5] and over-neutralization [6], leading to a radially increasing function f. For electron beam welding applications, the loss of ion neutralization by fast beam deflection and its influence on the focusing properties have been investigated by Dilthey *et al.* [7]. An arbitrary radial distribution of electrons has been used by Zapalac [8] to study the change of beam profiles by transport and focusing. The initial distribution used, however, is not a self-consistent solution of the problem.

In this paper we present self-consistent solutions that are particularly useful in the area of EBIS and EBIT devices, especially for those working without magnetic field [9,10]. These solutions will be used in a forthcoming paper to investigate the matching conditions for the beam entering into the pinched ion trap region.

II. NUMERICAL MODELING

We consider an electron beam in which the beam spreading by space charge and finite emittance is balanced by the inward forces due to the self-magnetic field and the presence of ions. The beam is propagating through a conducting tube polarized—with respect to the cathode—to the accelerating potential. We also assume that the tube contains per unit of length the same amount of beam and neutralizing particles, which is met by Bennett's analytic solution only for very low energies. In our more general and realistic case, the electrical field strength vanishes towards the tube wall. This may be called full neutralization (or compensation), although there still exist radial fields inside the beam and between the beam and the tube, due to the different radial distribution of electrons and ions.

A. Parameters and equations

Two components will be considered: fast electrons and slow ions. The first ones are emitted by a uniform circular cathode with current I, accelerated to an axial velocity $v_z = \beta c$, and creating a charge density distribution $\rho_e(r)$ of cylindrical symmetry for which a Maxwellian distribution of transverse velocities, characterized by a temperature T_e, is a good approximation. As a result of ionizing

*On leave from Dept. Física Aplicada III, Facultad de Física, UCM, E-28040 Madrid, Spain.

collisions with gas molecules, positive ions are born in the radial potential well of the electron beam. Oscillating in this well, the ions thermalize by mutual collisions much faster than neutralization occurs. By the increasing amount of ions, the electronic space charge becomes partially compensated and the radial potential decreases, ending in a stationary state characterized by a temperature T_i and an ion density distribution $\rho_i(r)$, in which the generation of ions is balanced by their radial loss to the wall. In the present treatment T_i is taken as a free parameter because it is dependent on many experimental details, such as vacuum pressure, gas composition, electron current density, electron energy, potential on trapping electrodes, etc., which need to be considered in applying our results.

The amount of ions lost in the time of thermalization is considered to be much lower than the amount trapped, which permits one to apply the Boltzmann assumption for the spatial adjustment of thermal ions to the potential. Secondary electrons generated by ionization are expelled from the beam region by the radial electric field as well as by the "Coulomb wind" of the primary beam in the axial direction as found in the operation of many EBIS devices. The steady-state potential distribution $U(r)$ and the particle densities are related through Poisson's equation

$$\Delta U(r) = \frac{\partial^2 U}{\partial r^2} + \frac{1}{r}\frac{\partial U}{\partial r} = -\frac{\rho_e + \rho_i}{\varepsilon_0}, \tag{2.1}$$

where ε_0 is the vacuum permittivity. The Boltzmann assumption for either type of particles gives

$$\rho_e = \rho_{e0}\exp\left[-\frac{q_e[U_e(r) - U_e(0)]}{kT_e}\right], \tag{2.2a}$$

$$\rho_i = \rho_{i0}\exp\left[-\frac{q_i[U(r) - U(0)]}{kT_i}\right], \tag{2.2b}$$

where ρ_{e0} and ρ_{i0} are the charge densities at the beam center, $q_e = -e$, where e denotes the elementary charge, and $q_i = q^* e$ for q times charged positive ions. U_e is the effective potential for the electrons, explained below.

An analytic solution can be readily obtained for the case of a cold beam and in absence of ions, which we quote for reference. Thus, for the distribution

$$\rho_e(r) = \begin{cases} \rho_0, & 0 \le r \le r_b, \\ 0, & r_b < r \le r_t, \end{cases} \tag{2.3}$$

the potential difference between the center and the beam edge is given by

$$\delta U = U(r_b) - U(0) = -\frac{\rho_0 r_b^2}{4\varepsilon_0} = \frac{I}{4\pi\varepsilon_0\beta c}. \tag{2.4}$$

From this solution we define f_e and f_i to relate to the axial densities in Eqs. (2.2) as

$$\rho_{e0} = f_e\rho_0, \tag{2.5a}$$

$$\rho_{i0} = -f_i\rho_0 \tag{2.5b}$$

and introduce further dimensionless parameters to describe the temperatures of electrons and ions,

$$\mu_e = -\frac{q_e\delta U}{kT_e}, \tag{2.6a}$$

$$\mu_i = \frac{q_i\delta U}{kT_i}, \tag{2.6b}$$

which provide a convenient normalization to our problem. μ_e may have a wide range of values depending on the current, energy, and temperature of the electron beam, as seen in Table I. The beam temperature generally differs from the cathode temperature due to compression or decompression taking place in between. We can now write the Boltzmann assumptions as

$$\rho_e = f_e\rho_0\exp\left[\mu_e\frac{U_e(r) - U_e(0)}{\delta U}\right], \tag{2.7a}$$

$$\rho_i = -f_i\rho_0\exp\left[-\mu_i\frac{U(r) - U(0)}{\delta U}\right]. \tag{2.7b}$$

Values of f_e greater than 1 would imply a compression of the beam with respect to the uniform beam, a feature that is especially interesting in the application of neutralized relativistic electron beams.

A particular solution of Eq. (2.1) with distributions according to Eqs. (2.2) has been given by Bennett in the form

$$\rho_{e,i}(r) = \frac{\rho_{e,i}(0)}{[1 + r^2/a^2]^2}, \tag{2.8}$$

where a is the width parameter. The general feature of this solution is a constant degree of neutralization

TABLE I. Values of the temperature parameter μ_e [Eq. (2.6b)] of the electrons in dependence of beam current and energy. At $kT_e = 1$ eV these values correspond to the potential depression δU of the uniform beam [Eq. (2.4)].

U_t (keV) \ I (A)	0.0625	0.125	0.25	0.5	1	2
25	6.208	12.415	24.830	49.661	99.321	198.642
50	4.540	9.081	18.161	36.322	72.644	145.288
100	3.418	6.836	13.671	27.342	54.685	109.369
200	2.695	5.390	10.779	21.558	43.116	86.232
400	2.263	4.527	9.053	18.106	36.212	72.425
800	2.035	4.069	8.138	16.277	32.554	65.108

$f_B = -\rho_i(r)/\rho_e(r)$ throughout the beam that, for ions at rest or with low axial velocity, can be expressed as

$$f_B \cong \frac{\mu_i + \mu_e}{\mu_i + \gamma^2 \mu_e}, \tag{2.9}$$

where $\gamma = (1 - \beta^2)^{-1/2}$. It is seen that this quantity will always be less than 1, and, hence, Eq. (2.8) will not apply to completely neutralized electron beams.

B. The effective potential equation

The equation for the effective potential acting on a Boltzmann distribution of the beam particles is obtained from the radial force exerted on an electron of that beam,

$$m\ddot{r} = -q_e \frac{\partial U_e}{\partial r}. \tag{2.10}$$

Electrons and ions establish a radial electric field by their space charge, and an azimuthal magnetic field is created by the axial movement of the electrons,

$$m\ddot{r} = q_e\{E_r(r) - \nu_z B_\varphi(r)\}, \tag{2.11}$$

so that

$$U_e(r) = -\int_0^r [E_r - \nu_z B_\varphi]\, dr'. \tag{2.12}$$

The expressions for the electric and magnetic field distributions are easily obtained by applying the laws of Gauss and Ampère, respectively. Hence, the effective potential at any radial position r can be calculated as

$$\begin{aligned} U_e(r) &= -\frac{1}{\varepsilon_0}\int_0^r \frac{1}{r'}\left[\int_0^{r'} \{\rho_e(1-\beta^2) + \rho_i\} r''\, dr''\right] dr' \\ &= -\frac{1}{\varepsilon_0}\int_0^r \frac{1}{r'}\left[\int_0^{r'} \{\rho_e(1-\beta^2 - f)\} r''\, dr''\right] dr', \end{aligned} \tag{2.13}$$

where $f(r) = -\rho_i(r)/\rho_e(r)$ represents the local degree of space charge neutralization. It is worth noting that we can write a similar expression for the electrostatic potential by eliminating the term β^2, as inferred from Eq. (2.12).

C. Numerical algorithm for searching solutions

In solving Eq. (2.1) we are dealing with a steady-state problem which is, in essence, nonlinear. A considerable number of mathematical approaches can be used in its solution [11]. We have chosen a finite difference scheme that proved to be very efficient, provided some well-defined strategies were applied in the iteration process. The successive steps to obtain a self-consistent solution can be summarized as follows.

(i) Define, as input parameters and starting values, the beam current I, the axial velocity ν_z, the radii of the beam r_b and of the tube r_t, the applied accelerating potential U_t, and the temperatures of the electrons and of the compensating ions through parameters μ_e and μ_i. Provide a grid to define potentials and space charges in 1000, 2000, 4000, and 8000 radial positions, and prescribe control parameters to assure convergence.

(ii) Solve Poisson's equation by iteration, using under-relaxation, performing the following substeps:

(a) Initialize densities with approximate distributions. [Sometimes, box-shaped solutions of the type given in Eqs. (2.3) were accepted to start the iteration, but, also, former solutions of neighboring parameters could be loaded from a file.]

(b) Determine the potential distribution $U(r)$ and the corresponding $\rho_i(r)$. (To solve the linear tridiagonal system of equations resulting from the finite difference scheme, a fast solver based on Crout reduction was used.)

(c) Sum the total positive charge and adjust ρ_i to get the required degree of neutralization.

(d) Repeat (b) and (c) until differences in the potential at all points of the grid compared to the values of the previous iteration are less than a pre-fixed tolerance (typically 10^{-6}).

(e) Calculate the effective potential $U_e(r)$, as given in Eq. (2.13), and the corresponding electron density $\rho_e^*(r)$.

(f) Compute new ρ_e using the under-relaxation formula

$$\rho_e^k = \frac{\rho_e^{k-1} + w\rho_e^{*k}}{1 + w}, \tag{2.14}$$

where w is a factor controlling the weight of ρ_e^* in the construction of the new distribution, being increased continuously from 0.01 to 1 as the number of iterations k increases.

(g) Correct the new ρ_e in order to keep I constant.

(h) Repeat steps (b) to (g) until the desired convergence is achieved.

We found a great variety of solutions in dependence of the most relevant parameters to our problem, that is, the energy of the beam and the temperature of both kinds of particles. Emphasis has been given to explore the range of parameters where the region of convergence is neighboring the region for nonconverging solutions. In addition, we also succeeded in reproducing the analytic solution of Bennett [1] in the appropriate range of parameters, which may be considered as a valid test for the developed numerical procedures.

III. RESULTS AND DISCUSSION

In this section we present some typical solutions of the Poisson equation for a cylindrical electron beam subjected to the boundary condition $U(r_t) = U_t$ and to full neutralization by singly charged ions $E_r(r \to r_t) \to 0$. In all cases the beam current has been set to $I = 1$ A and $r_b = 0.1 r_t$. Results of the calculations are given in Figs. 1 and 2. For each set of parameters, the corresponding solutions are presented in two panels: Figs. 1(a) and 2(a) show the normalized electrostatic and effective potentials, and Figs. 1(b) and 2(b) show the spatial distribution of

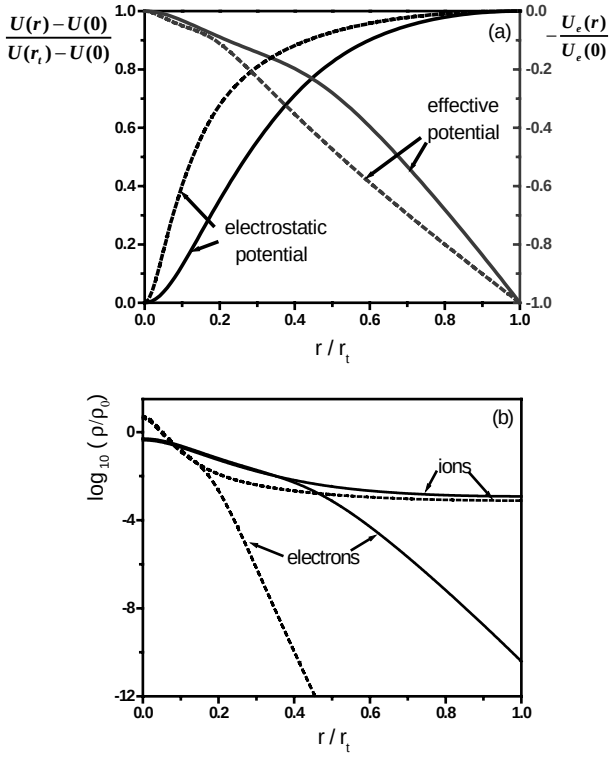

FIG. 1. Radial functions for (a) electrostatic and effective potentials and (b) space charge of electrons and ions, calculated for a 50 keV electron beam and neutralizing ions with a temperature related to $\mu_i = 11.5$. Full lines correspond to hotter ($\mu_e = 114$) electrons and dashed lines to colder ($\mu_e = 201$) electrons.

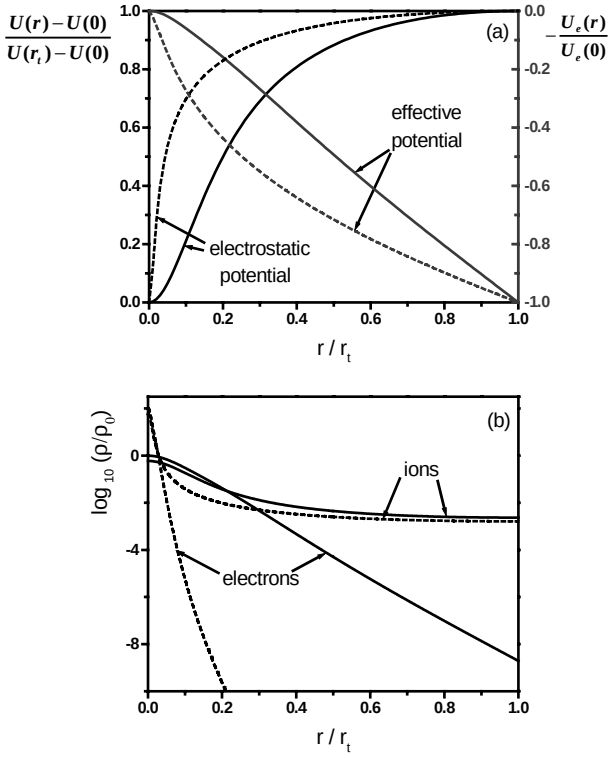

FIG. 2. Radial functions for (a) electrostatic and effective potentials and (b) space charge of electrons and ions, calculated for a 200 keV electron beam and neutralizing ions with a temperature related to $\mu_i = 4$. Full lines correspond to hotter ($\mu_e = 20$) electrons and dashed lines to colder ($\mu_e = 31$) electrons.

electrons and ions, both normalized to the density of the uniform beam. The parameters have been selected to exhibit solutions with low (solid lines) and high (dashed lines) compression. The general shape of the space charge functions reflects the action of the potentials on the Boltzmann distribution. Full neutralization provides the vanishing derivative of the potentials at the tube wall and the crossing of electronic and ionic space charges at an intermediate radius. This crossing radius is smaller for higher compressions and higher energy and corresponds to the differences of f_e and f_i. Near the axis, these functions seem to be parallel in the logarithmic presentation resembling the feature of Bennett's analytic solutions.

Figures 3(a)–3(c) illustrate the dependence of the electron compression at the axis f_e and of the central degree of neutralization $f(0) = f_i/f_e$, for three different energies and for different combinations of the parameters μ_e and μ_i. We observe at all energies a similar behavior: for constant μ_e an increase of μ_i leads to higher values of both quantities, which is explained by a higher neutralization, because the ions become colder, allowing the electron beam to pinch more. Increasing μ_e at constant μ_i, however, will give a higher value of f_e, caused by the reduced emittance of colder beams, and slightly diminishes f_i/f_e. It is also important to note that, as we go to the left and upper regions in these figures, the regime is becoming more and more nonlinear up to the point that either it is not possible to reach convergence (left region) or any small variation of the parameter μ_e is producing an enormous change in the value of f_e (upper region). For these cases, meshes with 8000 points were provided to assure a correct solution, which was also confirmed by extrapolating the results from calculations with 1000, 2000, and 4000 points.

An overview on the regions of the fundamental parameters (U_t, μ_e, and μ_i) in which we have found solutions of interest is presented in Fig. 4. The lower curves (dashed) belong to $f_e = 1$, and the upper ones (solid) belong to points for which convergence due to the nonlinear behavior became troublesome. Below the dashed lines are regions of low compression, and to the right end of each pair, $\mu_e \gtrsim \mu_i$, no solutions can be obtained, because our requirement of full neutralization forces the ions to be hotter than the electrons in order to be more abundant at larger radii, as seen in Figs. 1(b) and 2(b). We also notice that higher values of μ_e and μ_i are needed to obtain compression by pinching at lower energies. In experiments it will become more and more difficult to observe this effect at values of $\beta \ll 1$.

We have further looked for the reproduction of Bennett's analytic solution as given in Eq. (2.8). In this case it will be necessary to relax the condition of full neutralization. We

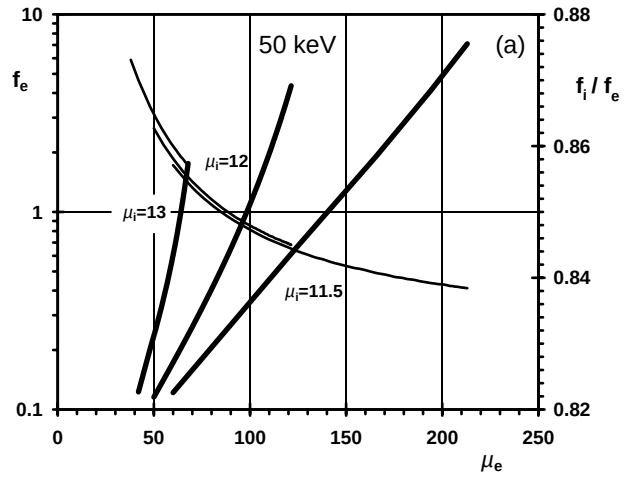

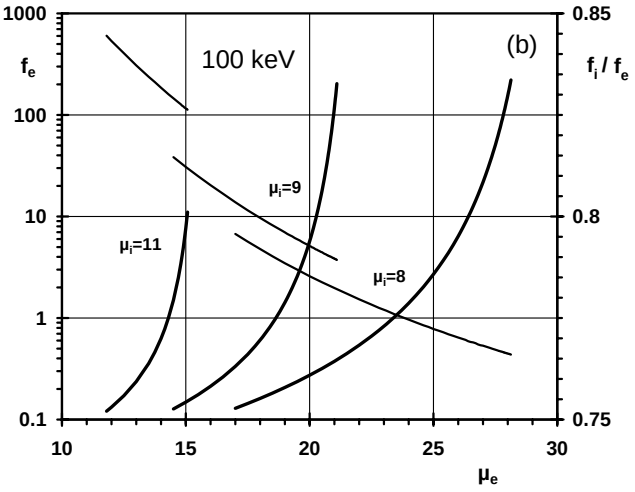

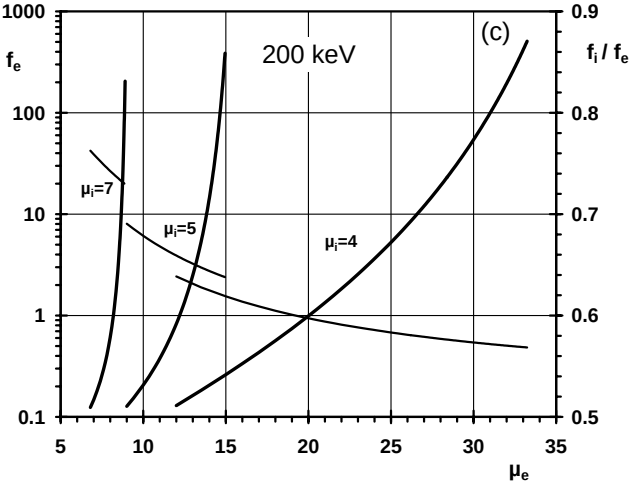

FIG. 3. Variation of the central electron compression f_e (thick lines) and of the central degree of neutralization f_i/f_e (thin lines), as functions of the parameters μ_e and μ_i for beam energies of (a) 50 keV, (b) 100 keV, and (c) 200 keV. For colder beams (increasing μ_e), higher compression at lower central neutralization becomes possible. At lower energies, where the pinching is less effective, colder electrons and ions are required to obtain self-consistent solutions.

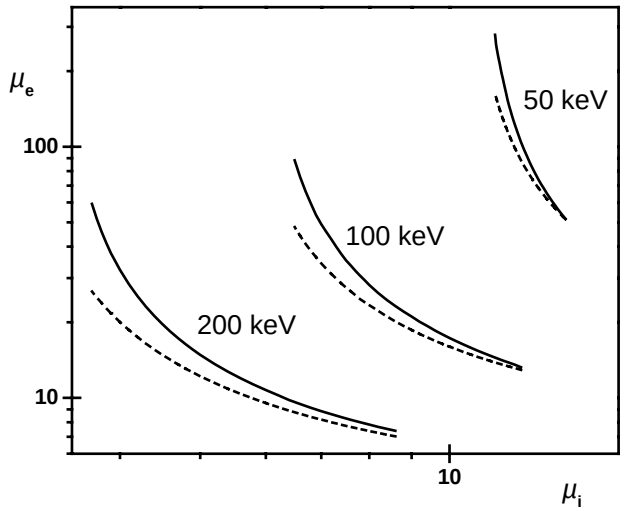

FIG. 4. Range of temperature parameters μ_e and μ_i for which stable solutions can be found at the studied energies. The solid curves are at the limit of stability with high beam compression; below the dashed curves the beam will be decompressed ($f_e < 1$).

first calculated three cases for 50, 100, and 200 keV, choosing μ_i and μ_e such that $f_e = 5$ resulted for the neutralized beam (any other choice will lead to similar conclusions). Next, the total amount of beam neutralization was reduced in small steps until no crossing was found in the radial falloff of the particle distribution functions. In Table II data are listed in order to compare our numerical results with Bennett's solutions. The computed distributions can be well fitted to functions as described by Eq. (2.8) with larger width for higher energies, coinciding within $10^{-6}\%$ near the axis and 0.2% near the tube wall. At lower energies, Bennett's relation (2.9) for f_B is well reproduced by the ratio f_i/f_e of our solutions, while at higher energies the discrepancy gets larger. This may be due to the increase of the width parameter a, by which the differences between Bennett's unbounded and our bounded solutions are becoming more apparent at these energies.

Finally, we note that when ν_z is also small compared with the velocity of light, both approaches will lead to

TABLE II. Comparison of Bennett's solutions with numerical solutions at arbitrarily selected parameters: a/r_t is the relative width obtained by fitting the space charge distributions to Eq. (2.8). The values of f_e indicate decompression, and the central neutralization factor f_i/f_e should be compared to Bennett's f_B in Eq. (2.9).

	Energy (keV)	50	100	200
Preset parameters	μ_i	11.5	8.0	4.0
	μ_e	201	25.7	24.8
Numerical results	a/r_t	0.282	0.300	0.448
	f_e	0.138	0.121	0.060
	f_i/f_e	0.839	0.771	0.584
Bennett	f_B	0.837	0.753	0.554

a "complete solution" of the Poisson's equation giving the same amount of negative and positive charges along the radial direction, $f_B = f \cong 1$. This solution, however, has lost all appealing features of compensated relativistic beams.

IV. SUMMARY

We have reported a method and presented the results on self-consistent solutions of the radial functions of space charge and potential for a relativistic electron beam with transverse thermal velocities neutralized by ions with a thermal energy distribution. In a wide range of parameters we have found well converged solutions but also limits of existence, for energies of 50, 100, and 200 keV. High compressions of the electron beam are obtained for higher energies and colder electron beams. A unique feature of all solutions is the radial increase of the neutralization factor. In contrast to the well-known analytic solution of the Bennett's pinch, we have assumed a complete neutralization, i.e., same amount of positive and negative charges per unit beam length. By relaxing this condition, a reasonable agreement of our numerical simulations with Bennett's results is found, the discrepancies being due to the imposed boundary condition in our case.

Work is in progress to use these results for ray-tracing simulations from the neutralized to the non-neutralized region, thus providing (in reversed direction) the injection conditions for initiating this kind of flow.

ACKNOWLEDGMENT

One of the authors, G. M., is grateful to the Spanish Ministerio de Educación y Cultura for support.

[1] W. H. Bennett, Phys. Rev. **45**, 890 (1934).
[2] G. I. Budker, Sov. J. At. En. Z **147**, 673 (1956).
[3] J. D. Lawson, *The Physics of Charged-Particle Beams* (Clarendon, Oxford, 1988), pp. 200–206.
[4] R. E. Rand, M. C. Lampel, and D. Y. Wang, J. Appl. Phys. **62**, 1639 (1987).
[5] R. Becker, Nuovo Cimento Soc. Ital. Fis. **106A**, 1613 (1993).
[6] S. P. Sabchevski and G. M. Mladenov, J. Phys. D **27**, 690 (1994).
[7] U. Dilthey, S. Böhm, A. Goumeniouk, T. Welters, O. K. Nazarenko, and K. S. Akopjanz, International Institute of Welding, Paris, IIW Doc. No. IV-702-98, 1998.
[8] G. H. Zapalac, Phys. Rev. ST Accel. Beams **2**, 114201 (1999).
[9] R. Becker, E. D. Donets, M. Kleinod, H. S. Margolis, and J. D. Silver, Rev. Sci. Instrum. **67**, 983 (1996).
[10] M. Mücke, R. Rao, R. Becker, and M. Kleinod, Rev. Sci. Instrum. **69**, 691 (1998).
[11] A. Iserles, *Numerical Analysis of Differential Equations* (Cambridge University Press, Cambridge, England, 1996), Chaps. 7–12.